

SYNOPTIC ANALYSIS OF THE PERTURBATION OF AN OVERRUNNING CURRENT BY THE INTRUSION OF COLD AIR

MASAMICHI OI

Institute of Meteorology, Osaka Gakugei University, Osaka, Japan

and

MITSURU SEKIOKA

Institute of Meteorology, Defence Academy, Yokosuka, Japan

ABSTRACT

An actual three-dimensional analysis and the corresponding theoretical computation show that a cold air tongue intruding southward about the middle of January 1956 along the eastern side of the Rocky Mountains causes the overrunning warmer current to curve convexly toward the lower pressure side. The current behaves similarly to flow over terrestrial topography of the same shape. Moreover the results indicate that a cold air dome can produce perturbations as large as those produced by the Rocky Mountains.

1. INTRODUCTION

One of the authors, Oi [3, 4], citing Elliott's [1] schematic illustration, has stated that a shallow tongue of cold air influences the overrunning warm zonal current as does the terrestrial topography. However, this was quite speculative, as was Elliott's schematic description of the perturbation of the upper zonal current pattern by the outbreak of polar air, or Panofsky's [7] statement that the cold air dome behaves as a barrier to the overrunning current to form a trough downstream. It seems to us that none of these statements about a cold air barrier has been substantiated by three-dimensional synoptic analysis. To analyze three-dimensionally the perturbation of an overrunning current caused by the shallow tongue of underlying cold air, we started, at first, to use the synoptic data [10] at hand over the Far East. We discontinued the analysis over this region, however, because the amount of data, especially the upper air data over China, is not adequate to figure out the three-dimensional perturbation.

We then selected the North American Continent as a region of analysis for our purpose. The North American network of radio-soundings is comparatively dense and uniformly distributed, although its west-east extent is rather narrow. Scanning the 500-mb. and sea level maps [10] from 1955 to 1956 for a case suited for the purpose of this analysis, we found, seemingly, only one spell, a period in January 1956 during which a shallow tongue of cold air persistently crept southward with a well-defined overrunning warm current. To figure out the perturbation of the zonal westerlies overrunning the shallow tongue of cold air, we constructed trajectories of air parcels within both air masses—underlying cold and overrunning warm—and made a three-dimensional synoptic analysis of the

behavior of the zonal westerlies as the cold air intruded southward slowly and persistently. The data used for this analysis are all from [10].

As far as we searched, we found that this type of case does not often form; we more often found cases such as Palmén and others [2, 5, 6] treated, in which the cold air extends from the ground to the stratosphere and protrudes southward uniformly through the whole layer from bottom to top without any overrunning warm southerly zonal current.

The data for the case reported here are restricted to a certain spell during one winter, mid-January, 1956. With more adequate data, analogous examples might be found at other dates or in many other regions, even on the oceans. However, we now restrict ourselves to this one example, mainly because of our limited time and manpower.

2. METHODS OF ANALYSIS

First, we drew on the 850-mb., 700-mb., and 500-mb. surfaces the frontal contours during the period of analysis so as to visualize the southward displacement of the frontal surface enveloping the cold air tongue in the lower layer. Next, we had to determine whether this southward displacement is an actual cold air intrusion or a fictitious one—for instance, there might be seen some frontal characteristics produced by radiational cooling or other causes. For this purpose, we selected several parcels in the lower cold air and obtained the position of each parcel at consecutive 12-hr. intervals by Petterssen's [9] method under the assumption that the parcels conserved potential temperature. Of course the isentropic trajectories which we adopted deviated somewhat from the actual trajectories. Because we could not find any

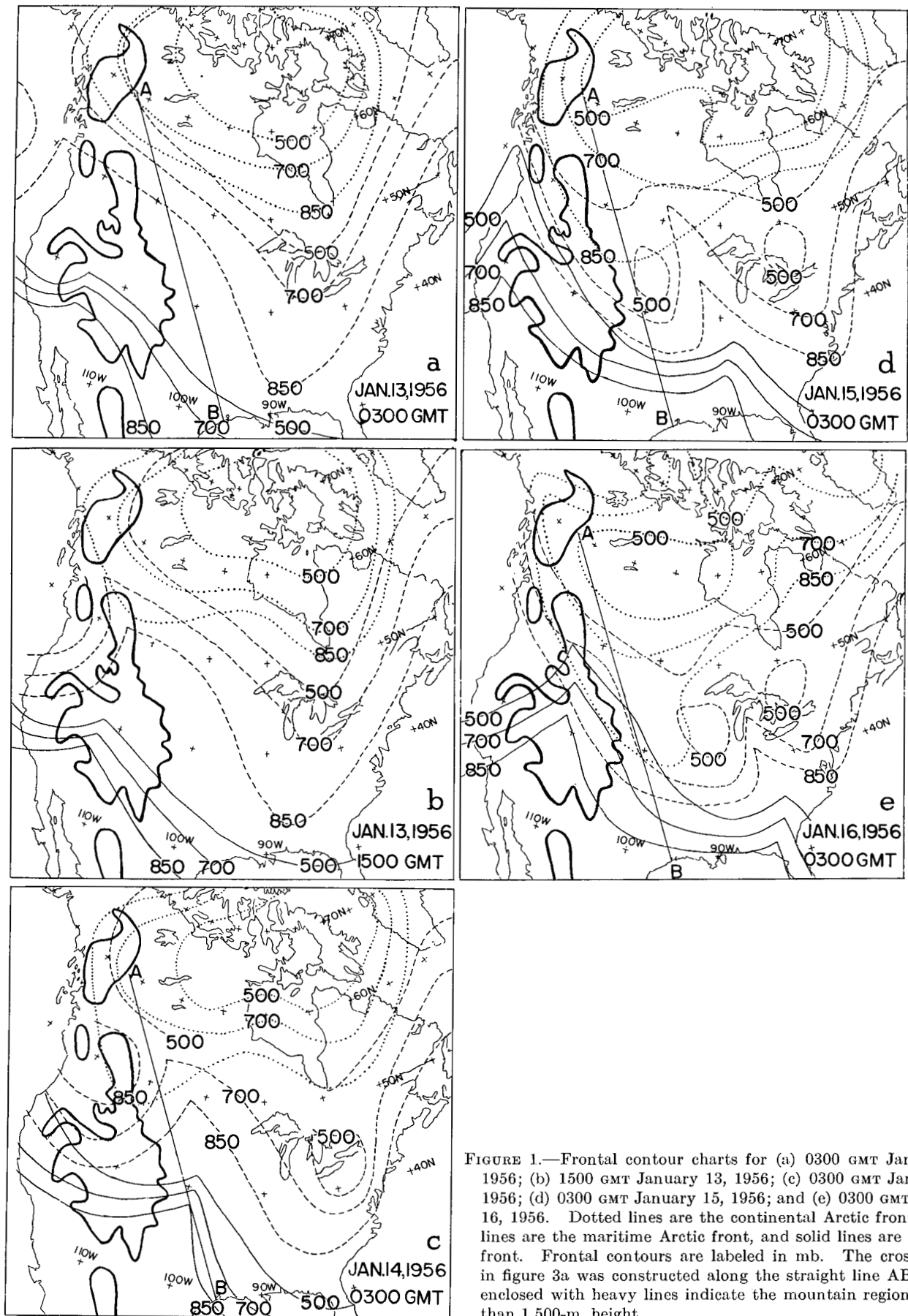


FIGURE 1.—Frontal contour charts for (a) 0300 GMT January 13, 1956; (b) 1500 GMT January 13, 1956; (c) 0300 GMT January 14, 1956; (d) 0300 GMT January 15, 1956; and (e) 0300 GMT January 16, 1956. Dotted lines are the continental Arctic front, dashed lines are the maritime Arctic front, and solid lines are the polar front. Frontal contours are labeled in mb. The cross section in figure 3a was constructed along the straight line AB. Areas enclosed with heavy lines indicate the mountain region of more than 1,500-m. height.

better way to proceed, we used this isentropic method even though it seemed somewhat semi-quantitative.

To make clearer the vertical structure of the cold air tongue and overrunning air, we constructed the vertical cross sections along the direction of progression of the cold air tongue. Here we adopted the geometric height¹ in order to fix the height of terrestrial topography. The air mass overrunning the cold air tongue was mA air in the northern part of the region of concern and mP air in the southern part. We drew isentropic trajectories of these parcels similarly as we had for the cold air parcels.

The trajectories of air parcels overrunning the cold air tongue were influenced not only by the cold air tongue itself but also by terrestrial topography lying near—i.e., the Rocky Mountains. Therefore, we could not compute the effect of the cold air tongue alone, which was our purpose, by the trajectories as constructed. To eliminate this terrestrial effect in the trajectories, we constructed air trajectories influenced only by the terrestrial topography (i.e., without any underlying cold air tongue) during a similar flow situation preceding and following the period of the cold air intrusion. In addition, to do this comparison synoptically, we found among the Normal Weather Charts [11] a monthly mean chart for which the zonal index value equaled the mean during the period of cold air intrusion and took its contours over the region as the air trajectories influenced only by the terrestrial topography. Finally, perturbations due to the terrestrial topography only and due to both terrestrial and aerotopographical barriers were obtained and compared by a theoretical computation for a zonal current with the same zonal index value.

3. RESULTS OF ANALYSIS

INTRUSION OF COLD AIR

Figures 1a–1e show the frontal contours at the 850-mb., 700-mb., and 500-mb. surfaces for January 13–16, 1956. The classification of air masses in this region is due to Penner [8]. Accordingly the fronts shown in these figures are, respectively from the north, the continental Arctic front between the cA air and the mA air, the maritime Arctic front between the mA air and the mP air, and the polar front between the mP air and the mT air.

In figures 1a–1e, the southward intrusion of the cA air along the east side of the Rocky Mountains can be seen only on the 850-mb. surface, but not on the 700-mb. and 500-mb. surfaces. On the other hand, the maritime Arctic front seen along the Pacific coast at 0300 GMT January 13 was displaced east-southeastward near the Great Lakes at 0300 GMT January 16 through the whole layer, overrunning the cA air intrusion in the lower layer.

In figure 2 are superposed the positions of the continental Arctic front at the 850-mb. surface during the

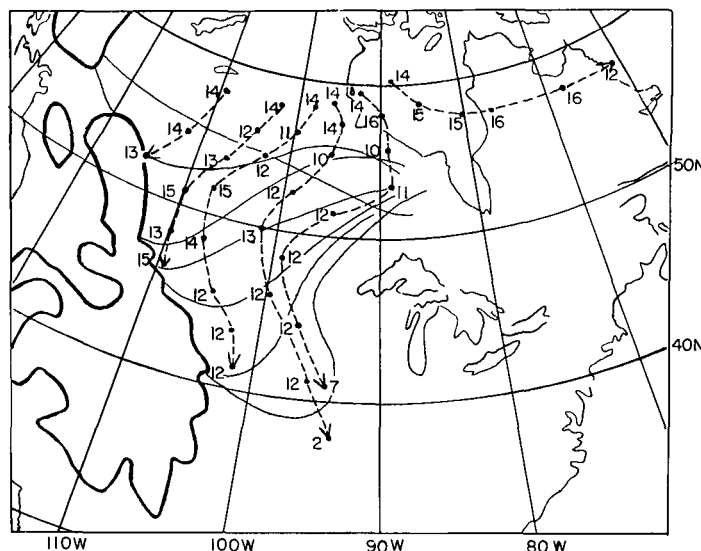


FIGURE 2.—Trajectories of the cA air on the isentropic surface $\theta = 264^\circ \text{A}$. from 0300 GMT January 13 (dashed lines). Heights corresponding to the positions of different air parcels are indicated in 100's of meters at 12-hr. intervals. Successive 12-hr. positions of the southward progressive continental Arctic front from 0300 GMT January 13 on the 850-mb. surface are shown by solid lines. Areas enclosed with heavy lines indicate the mountain region of more than 1,500-m. height.

period January 13–16 to indicate its gradual southward displacement. Also in this figure are shown the trajectories of six air parcels on the isentropic surface $\theta = 264^\circ \text{A}$. after 0300 GMT January 13; the heights of the six parcels at the initial time (all were 1,400 m. which was about the middle height of the cA-air layer, taken as representative of this layer); and their successive heights, labeled in 100's m. near their respective positions at 12-hr. intervals. In this figure we can see that the parcels moved southward while generally descending during the period. However, the path of the westernmost parcel, nearest the Rocky Mountains, seemingly had the general descending tendency of the others but simultaneously an ascending tendency from the effect of the mountain slope. The speed of southward displacement of each parcel was about 35 km./hr., a little faster than that of the front at the 850-mb. surface, and the direction of displacement was approximately the same as that of the front. The heavy lines in this figure enclose the regions higher than about 1,500 m. elevation² reached by some of the trajectories and beyond which they could not be extended because of the lack of data over the mountainous areas.

The two easternmost trajectories differed little in their locations at the beginning, but later became farther and farther apart. The difference in the locations at the end of the period became remarkably large as the easternmost parcel, instead of intruding southward, moved eastward, while the second parcel, which was at first located near

¹ The heights are given in g.p.m. or g.p.f., but we interpret them as geometric ones, since the error caused by this treatment is negligible for our purpose.

² cf. *The Oxford Atlas*, Oxford University Press, 1956.

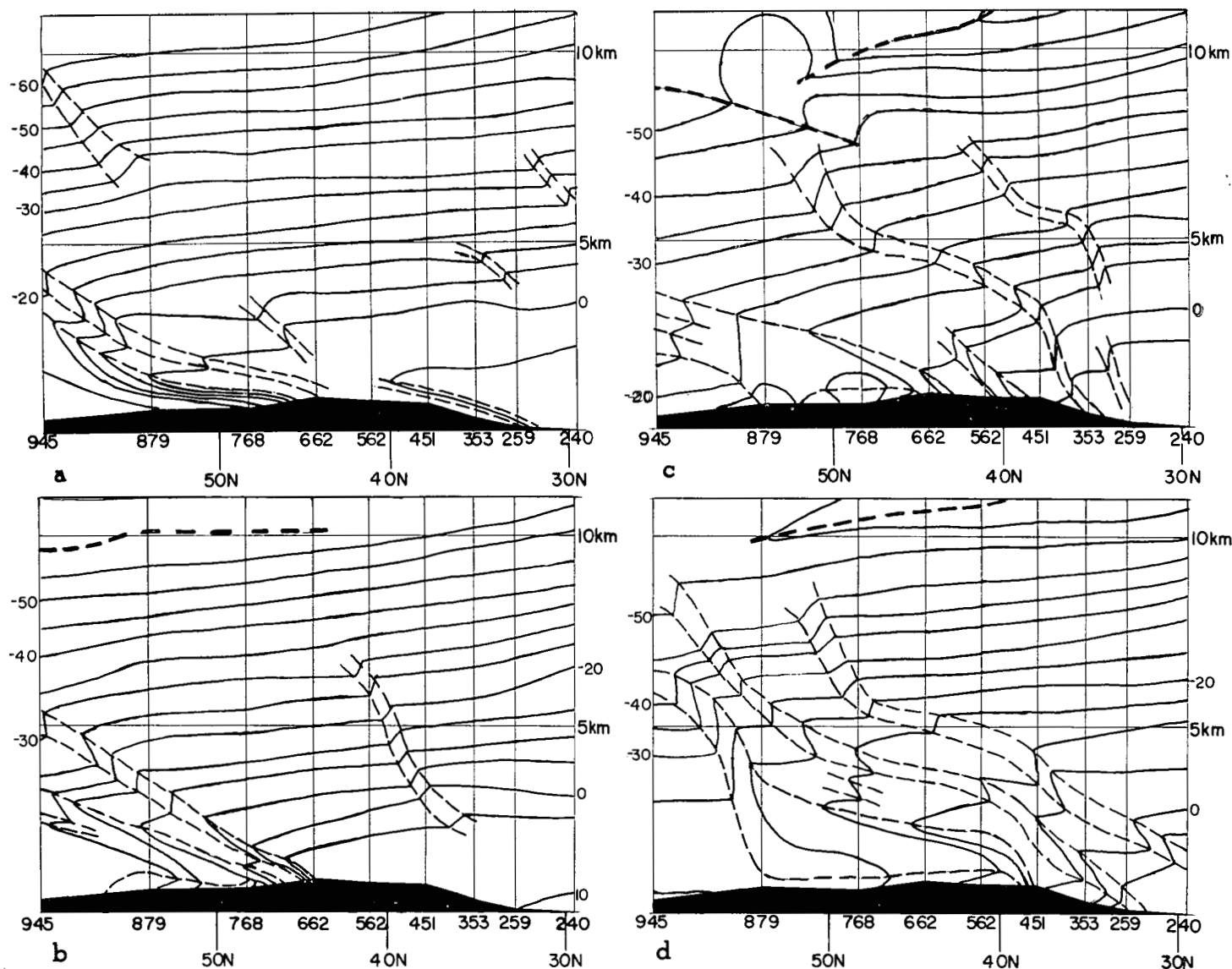


FIGURE 3.—Cross sections for (a) 0300 GMT January 13, 1956 along the line AB in figure 1a; (b) 0300 GMT January 14 along the line AB in figure 1c; (c) 0300 GMT January 15 along the line AB in figure 1d; (d) 0300 GMT January 16 along the line AB in figure 1e. Solid lines indicate isotherms in $^{\circ}\text{C}$. Dashed lines show the frontal and stable layers. Heavy dashed lines show the tropopause. Shaded area is the terrestrial topography. Vertical lines indicate the soundings used in the diagram with the international station numbers as follows: 945=Fort Nelson, British Columbia; 879=Edmonton, Alberta; 768=Glasgow, Mont.; 662=Rapid City, S. Dak.; 562=North Platte, Nebr.; 451=Dodge City, Kans.; 353=Oklahoma City, Okla.; 259=Fort Worth, Tex.; and 240=Lake Charles, La.

Churchill ($58^{\circ}45' \text{ N.}$, $94^{\circ}04' \text{ W.}$), moved southward. These circumstances corresponded to the fact that the eastern edge of the front at the 850-mb. surface approximately coincides with the 95° W. meridian.

The test sample of particle trajectories all started from an initial height of 1,400 m., as mentioned, but we can presumably consider that the parcels of the whole cA-air layer approximately followed analogous paths to those initially at 1,400-m. height.

Figures 3a–3d are the vertical cross-sections along a line connecting nine aerological stations from Fort Nelson ($58^{\circ}50' \text{ N.}$, $122^{\circ}35' \text{ W.}$) to Lake Charles ($30^{\circ}13' \text{ N.}$, $93^{\circ}09' \text{ W.}$) in the direction of displacement of the conti-

nental Arctic front for January 13–16. The cross-sections show that the lower cold air, which is to be analyzed mainly as an aerotopographical barrier with a slope of about $1/600$ and rather shallow average depth of about 2,000 m., gradually moved southward. As shown in figure 2, after 1500 GMT January 14, the trajectory of the third air parcel from west roughly coincided with the projection of this cross-section, and when we compare the height of this parcel with that of the upper limit of shallow cold air tongue, we recognize that this parcel always lay within the cold air domain.

The above analysis shows that the cold air was not produced by radiation cooling or other physical causes

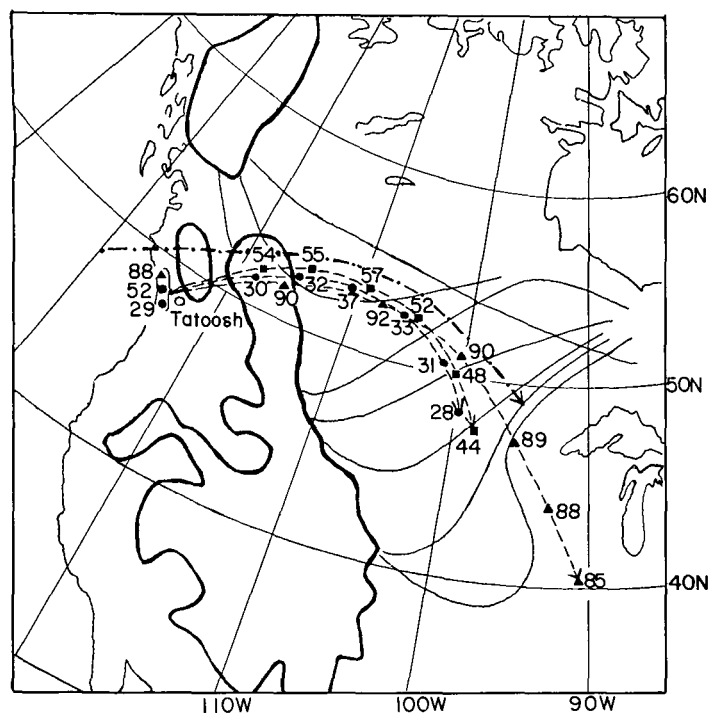


FIGURE 4.—Trajectories of the mA air on isentropic surfaces $\theta=317^{\circ}\text{A}$. (plotted as triangles), 293°A . (squares), and 286°A . (solid circles) from 1500 GMT January 13. Dashed and dotted line is theoretically computed streamline using the model topography of the Rocky Mountains and the cold air tongue as shown in figure 9a. (See legend for fig. 2.)

but very definitely was the southward intrusion of the cA air in the lower levels above the ground.

PERTURBATION OF OVERRUNNING ZONAL CURRENT

The maritime Arctic front shown in figures 1a–1e, overrunning the shallow tongue of the cA air, moved from the Pacific coast to near the Great Lakes in the period studied. Isentropic trajectories obtained by the method described above are shown in figure 4 for the air parcels with $\theta = 317^{\circ}\text{A}$, 293°A , and 286°A , lying near Tatoosh ($48^{\circ}23'\text{N}$, $124^{\circ}44'\text{W}$.) at 1500 GMT January 13 in the mA air region west of the front; and in figure 5 for the air parcels with $\theta = 307^{\circ}\text{A}$, 300°A , and 293°A lying at that time near Spokane ($47^{\circ}37'\text{N}$, $117^{\circ}31'\text{W}$.) in the mP air region east of the front. Although the scarcity of observing stations and the assumption of constant potential temperature might cause some errors, it is evident that these air parcels flowed convexly toward lower pressure over the cold air tongue and three parcels initially in the same vertical air column had approximately the same paths over the cold air tongue.

Moreover, figure 6 shows similar characteristics of trajectories of the mA air parcels lying near Tatoosh and Spokane at 0300 GMT January 14, 12 hr. later than the initial times in figures 4 and 5. Figure 6 suggests that the zonal current flowing over the cold air tongue was almost stationary. The heights of these parcels throughout their

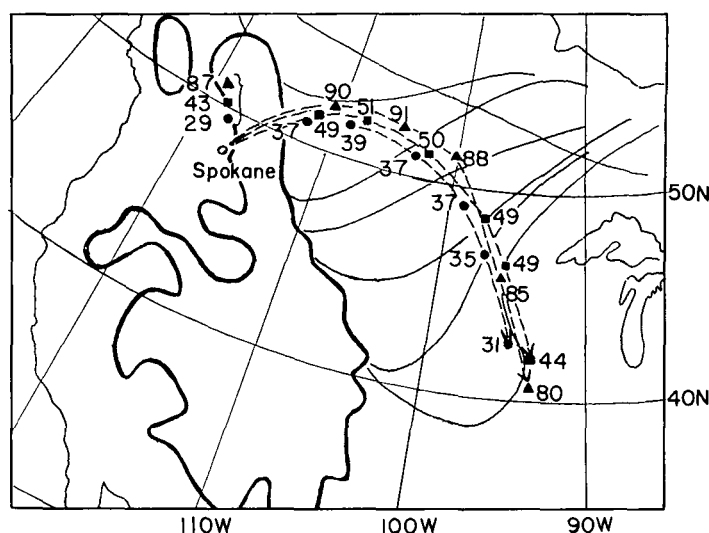


FIGURE 5.—Trajectories of the mP air on isentropic surfaces $\theta=307^{\circ}\text{A}$. (triangles), 300°A . (squares), and 293°A . (solid circles) from 1500 GMT January 13. (See legend for fig. 2.)

trajectories were always higher than the ridge of the cold air tongue and therefore, undoubtedly, these parcels flowed over the cold air tongue rather than penetrating the underlying cold air.

Also figure 6 shows for comparison the trajectories of the air parcel lying near Fort Nelson in the uniform cA air from upper to lower layer at 1500 GMT January 13 and of the mT air parcel then lying near El Paso ($31^{\circ}48'\text{N}$, $106^{\circ}24'\text{W}$), thus farther south than the cold air tongue had yet reached. The trajectories of these parcels, one in the northern part and the other in the southern part, both outside the region of the cold air tongue, uniformly spread eastward, which was entirely different from the above-analyzed trajectories over the region of the cold air tongue.

We may consider that this difference is mainly due to the underlying cold air tongue in the lower levels, although the difference caused by influences of the Rocky Mountains at different latitudinal belts is somewhat superimposed. Of course, without eliminating the influences of the Rocky Mountains, we can not give a strict discussion of the curving of the basic overrunning current due to the underlying cold air tongue.

To show the influence only of the Rocky Mountains upon the overrunning current, we present in figure 7 the trajectory of the mA air with $\theta = 286^{\circ}\text{A}$ during the period January 8–10, before the period of the intrusion of cold air. We can see that this trajectory was much less perturbed than those over the Rocky Mountains and cold air tongue shown in figures 4 and 5. For further confirmation, we adopted the following procedure. First, we obtained the zonal index values for each 5° latitudinal belt from 30°N to 60°N between 130°W and 90°W on the 500-mb. surface (see table 1). Next, from the normal 500-mb. charts [11], we selected the November

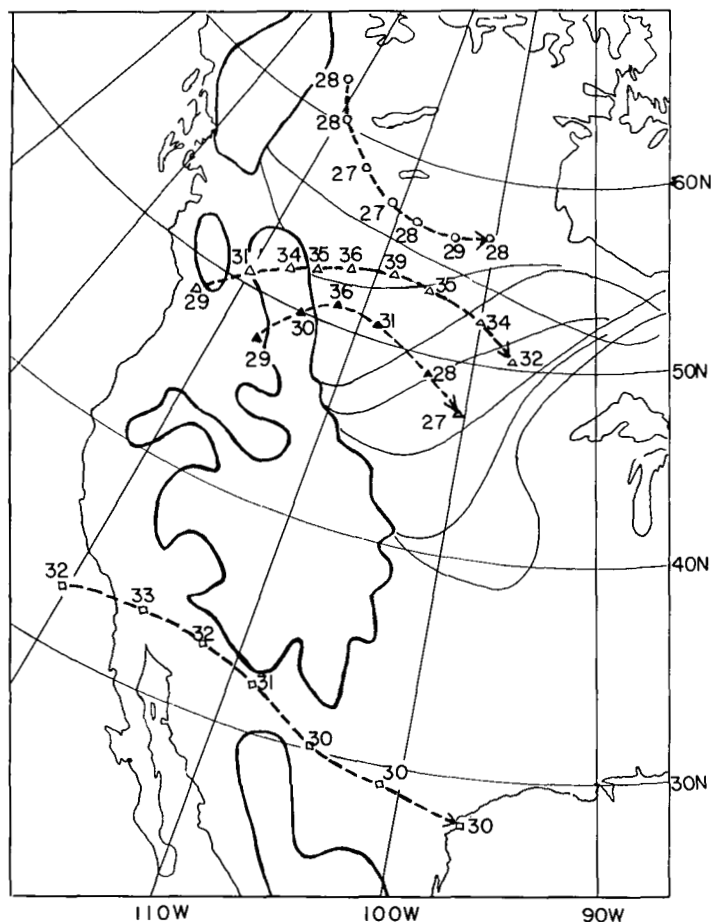


FIGURE 6.—Trajectories of different air parcels: the cA air on $\theta=275^\circ\text{A}$. surface from 1500 GMT January 13 (open circles); the mA air on $\theta=289^\circ\text{A}$. surface from 0300 GMT January 14 (open triangles); the mA air on $\theta=286^\circ\text{A}$. surface from 0300 GMT January 14 (solid triangles); and the mT air on $\theta=305^\circ\text{A}$. surface from 1500 GMT January 13 (open squares). (See legend for fig. 2.)

map (fig. 8) as most similar to the above-obtained zonal index distribution. The height of the overrunning current at $\theta=293^\circ\text{A}$. in figure 4 and at $\theta=300^\circ\text{A}$. in figure 5 was about 5,000 m. Consequently, we may consider the contours on the November normal 500-mb. chart as normal trajectories of air parcels influenced only by the Rocky Mountains. Figure 8 shows only a slight perturbation of these contours over the Rocky Mountains in the region of interest, as contrasted with the greater curvature of trajectories in figures 4 and 5.

Therefore, we conclude that the main cause of the trajectories' curving with greater amplitude over the

Rocky Mountains, as are seen in figures 4 and 5, was largely the influence of the underlying cold air tongue.

Although the cold air tongue was actually in a transient state of intrusion during the period, there almost certainly existed a mean bulk of cold air as an aerotopographical barrier. Then, since the overrunning current curved convexly toward the lower pressure side over the barrier, as we have seen above, we conclude that the cold air tongue played the same role as a mountain range, a role introduced by Oi [3, 4] as "aerotopography."

This is further verified by a comparison between the trajectories of air parcels shown in figures 4, 5, and 7 and the theoretically computed streamlines using the two-dimensional model barriers shown in figure 9 which was obtained by simplifying the terrestrial and aerotopographical cross-section along 50°N . latitude at 0300 GMT January 15 (see fig. 10) about the middle of the period of the cold air intrusion. Referring to the theoretical solution of Oi [3, 4], we can compute the trajectory overrunning the model barrier as follows:

The streamline (i.e., the trajectory in this case) is given by

$$\frac{dx}{u} = \frac{dy}{v}$$

$$u = \frac{U}{1 + \frac{1}{f} \frac{dv}{dx}}$$

$$v = \frac{g}{f} k^2 \sum_{n=1}^{\infty} (-1)^n \left[b_n \left(\frac{n\pi}{a} \right) \frac{(-1)^n \cos \frac{n\pi}{a} x - e^{-ak} \cosh kx}{\left(\frac{n\pi}{a} \right)^2 + k^2} - a_n \left(\frac{n\pi}{a} \right) \frac{(-1)^n \sin \frac{n\pi}{a} x}{\left(\frac{n\pi}{a} \right)^2 + k^2} + \frac{a_n \left(\frac{n\pi}{a} \right)^2 e^{-ak} \sinh kx}{k \left\{ \left(\frac{n\pi}{a} \right)^2 + k^2 \right\}} \right]$$

for $-a \leq x \leq a$,

where $f=2\Omega \sin \phi$ ($\phi=50^\circ\text{N}$. in this case) and a_n and b_n are harmonic constants for the topographical barrier $\xi(x)$:

$$\xi(x) \begin{cases} = \frac{a_0}{2} + \sum_{n=1}^{\infty} \left(a_n \cos \frac{n\pi}{a} x + b_n \sin \frac{n\pi}{a} x \right), & \text{for } -a \leq x \leq a \\ = 0, & \text{for } |x| \geq a. \end{cases}$$

In this computation, the following are adopted:

$n=15$ (which is sufficient to get the approximate value with small error)

$$k^2 = \frac{f^2}{gH - U^2} \cdot \frac{f^2}{gh}$$

H : height of the homogeneous atmosphere, 8 km.

g : acceleration of gravity, 9.8 m./sec.²

U : speed of original non-perturbed westerly current, 20 m./sec.

Thus, over the barrier ($-a \leq x \leq a$)

TABLE 1.—Height difference between 30°N . and 60°N . at the 500-mb. surface (100's of ft.)

Longitude ($^\circ\text{W.}$)	130	125	120	115	110	105	100	95
Mean value Jan. 12-16, 1956.....	15	16	16	16	17	17	16	16
November normal.....	15	15	16	16	17	17	17	18

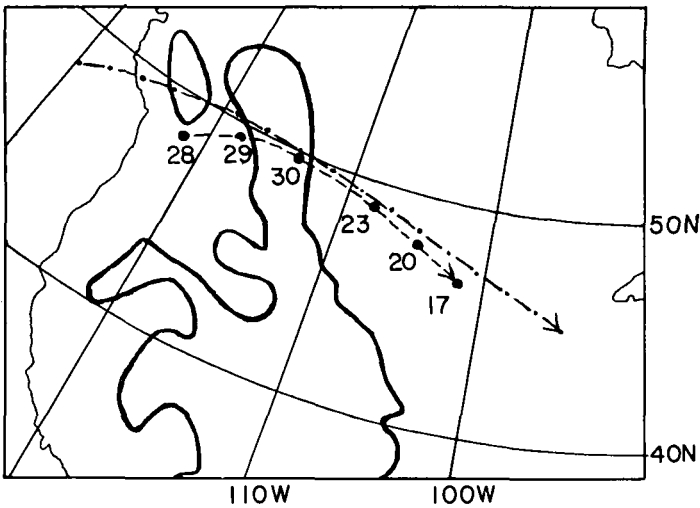


FIGURE 7.—Trajectories of the mA air on isentropic surfaces $\theta = 286^\circ$ A. from 0300 GMT January 8. Dashed and dotted line is theoretically computed streamline using the model topography of the Rocky Mountains as shown in figure 9a. (See legend for fig. 2.)

$$\begin{aligned} y(x) &= \frac{1}{U} \int_{-\infty}^x v dx + \frac{1}{2fU} [v^2(x) - v^2(-17.5l) + v^2(-17.5l)], \\ &\quad (\text{since } v(-\infty) = 0) \\ &= \frac{1}{U} \int_{-\infty}^{-17.5l} v dx + \frac{1}{U} \int_{-17.5l}^x v dx + \frac{1}{2fU} \\ &\quad [v^2(x) - v^2(-17.5l)] + \frac{1}{2fU} v^2(-17.5l) \end{aligned}$$

where $360\,l$ is the circumference of the latitudinal circle at 50° N. and a is the half width of the two-dimensional barrier, $17.5l$. The third term of the right-hand side was evaluated approximately at consecutive points $2.5l$ distance apart. The computed values of $v(x)$ and $y(x)$ with the two-dimensional model barrier $\xi(x)$ for the Rocky Mountains and superposed topographies as shown in figure 8b are given in table 2.

TABLE 2.—Values of v_R , v_S , y_R , and y_S , where l is the length of 1° of latitudinal circle at 50° N.; v_R is the N-S component of velocity due to the Rocky Mountains only; v_S is the N-S component of velocity due to the superposed topography; y_R is the y-coordinate of the trajectory from the foot of the model of the Rocky Mountains due to the Rocky Mountains only; and y_S is the y-coordinate of the trajectory from the foot of the model of the Rocky Mountains due to the superposed topography.

x	v_R m. sec. ⁻¹	v_S m. sec. ⁻¹	y_R (km.)	y_S (km.)
-17.5 <i>l</i>	10.02	16.16		
-15.0 <i>l</i>	9.80	16.51	87.55	148.48
-12.5 <i>l</i>	7.51	14.77	156.05	276.00
-10.0 <i>l</i>	4.41	12.21	201.01	381.08
-7.5 <i>l</i>	1.49	10.06	223.48	469.82
-5.0 <i>l</i>	-0.97	8.23	225.51	544.06
-2.5 <i>l</i>	-3.06	6.35	209.39	603.62
0.0	-4.82	3.64	177.27	641.62
2.5 <i>l</i>	-6.22	0.23	131.41	655.97
5.0 <i>l</i>	-7.29	-4.06	74.27	642.52
7.5 <i>l</i>	-8.02	-9.01	8.41	598.59
10.0 <i>l</i>	-8.43	-13.54	-63.57	520.76
12.5 <i>l</i>	-8.52	-16.37	-138.98	406.06
15.0 <i>l</i>	-8.31	-17.50	-214.97	263.31
17.5 <i>l</i>	-7.78	-16.97	-288.75	105.19

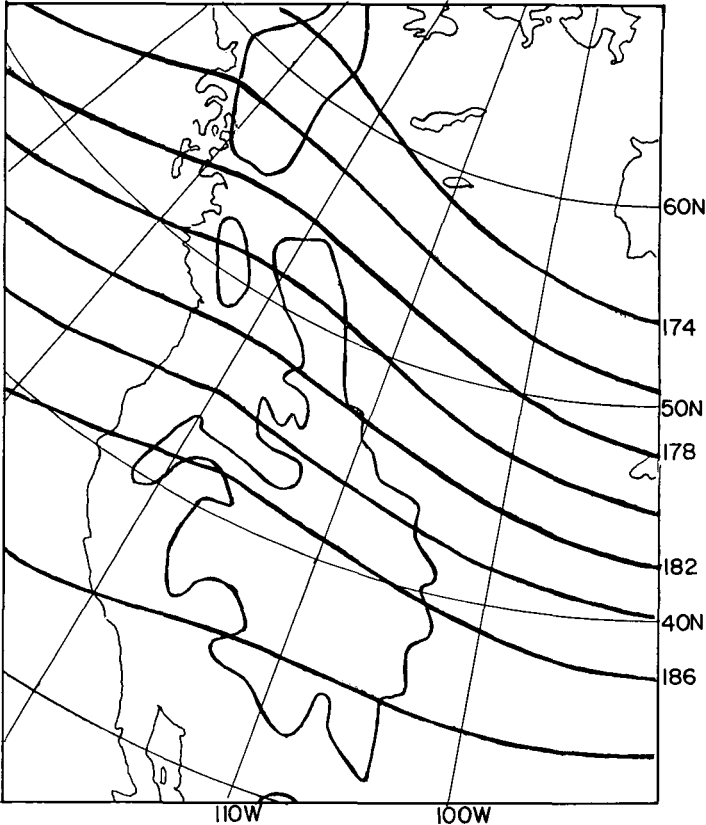


FIGURE 8.—Normal contours of 500-mb. surface for November [11]. Heights are shown in 100's of ft. Areas enclosed with heavy lines indicate the mountain region of more than 1,500-m. height

Trajectories thus obtained are superposed on figures 4, 5, and 7 for comparison with those synoptically analyzed. The computed trajectories are very similar to the synoptically analyzed ones. This evidence also strongly supports the suggestion that the aerotopography behaves as a barrier against the overrunning current similar to terrestrial topography of the same shape.

Since during the period of this analysis a disturbance was passing in the general leeside region of the cold air tongue, we could not verify the leeside “trough” downwind of the barrier pointed out by many authors. Moreover, with the lack of sufficient windward side data over the ocean, neither could we verify in detail the cyclonic curvature upstream and downstream from the barrier pointed out by Oi [3,4].

Finally the main air mass source which had been supplying the cA air for the southward intrusion was cut off by the warm air of the southern source region after about January 15 (see fig. 1d), and the area surrounded by the frontal contours on the 700-mb. and 500-mb. surfaces began to diminish. On the other hand, as shown by the 12-hr. consecutive positions of the Arctic continental front on the 850-mb. surface, the southward intrusion of the cold air tongue on this level reached the southernmost location on January 16 and then began to retreat northward to 50° N. on January 18. Also, since the front

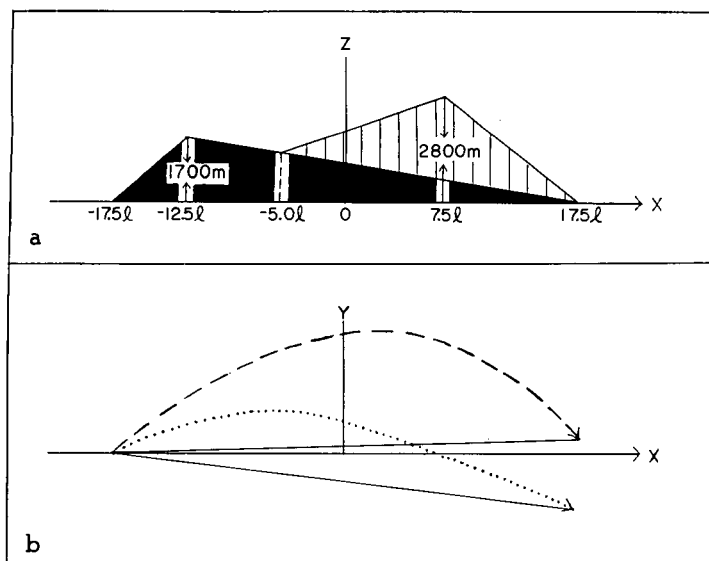


FIGURE 9.—(a) Model topography of the Rocky Mountains (shaded area) and the cold air tongue (hatched area) obtained by modification of figure 10. l is the length of 1° of latitudinal circle at 50° N. ($+17.5l$ indicates 95° W. and $-17.5l$ is 130° W.). (b) Theoretically computed streamlines. Dashed line is for overrunning the model of the Rocky Mountains and the cold air tongue, and dotted line is for overrunning the model of the Rocky Mountains only.

continued to move uniformly southward at sea level [10], we may conclude that this cold air tongue gradually diffused and disappeared while gradually decreasing its vertical extent.

4. CONCLUSIONS

We have found through the three-dimensional synoptic analysis of one example and a corresponding theoretical computation, the very interesting synoptic fact that a large-scale cold air intrusion causes the overrunning current to curve in the same sense and amount as terrestrial topography of the same shape causes.

As is clear from the present example, this kind of synoptic analysis is hampered by a scarcity of data; even for the continent of North America the extension of the observation network in the west-east direction is needed to overcome the scarcity of data over the oceans. Many more detailed analyses will be made when sufficient data become available. However, such phenomena as discovered in this study may take place in several regions of the globe and perhaps rather more often than we found in this example.

ACKNOWLEDGMENTS

The authors wish to thank Drs. R. D. Elliott, H. Panofsky, and J. K. McGuire for their kind information about the dates of syn-

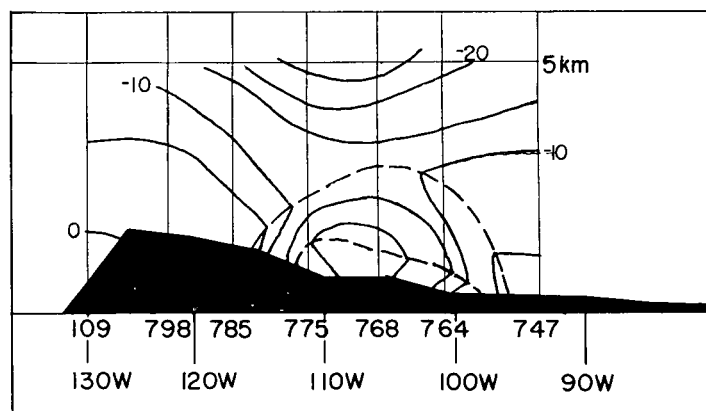


FIGURE 10.—Cross section for 0300 GMT January 15, 1956 along 50° N. (See legend for fig. 3a.)

optic data for cold air outbreaks and cold air domes in response to the authors' several inquiries. The authors also are very grateful to Mr. J. Namias for his kind suggestions on publishing this work.

REFERENCES

1. R. D. Elliott, "Extended Range Forecasting by Weather Types," *Compendium of Meteorology*, American Meteorological Society, Boston, 1951, pp. 834-840.
2. Y.-P. Hsieh, "An Investigation of a Selected Cold Vortex over North America," *Journal of Meteorology*, vol. 6, No. 6, Dec. 1949, pp. 401-410.
3. M. Oi, "Topographical Perturbation of a Zonal Current (Part 1)," *Memoirs of the Osaka University of the Liberal Arts and Education*, B, No. 5, 1956, pp. 16-31.
4. M. Oi, "Steady Topographical Perturbation of a Zonal Current," *Journal of Meteorological Society of Japan*, 75th Anniversary Volume, Nov. 1957, pp. 119-125.
5. E. Palmén and K. M. Nagler, "The Formation and Structure of a Large-Scale Disturbance in the Westerlies," *Journal of Meteorology*, vol. 6, No. 4, Aug. 1949, pp. 227-242.
6. E. Palmén and C. W. Newton, "On the Three-Dimensional Motions in an Outbreak of Polar Air," *Journal of Meteorology*, vol. 8, No. 1, Feb. 1951, pp. 25-39.
7. H. A. Panofsky, *Introduction to Dynamic Meteorology*, The Pennsylvania University, University Park, Pa., 1958, 243 pp. (p. 118).
8. C. M. Penner, "A Three-Front Model for Synoptic Analysis," *Quarterly Journal of the Royal Meteorological Society*, vol. 81, No. 347, Jan. 1955, pp. 89-91.
9. S. Petterssen, *Weather Analysis and Forecasting*, vol. 1, 2d edition, McGraw-Hill Book Co., Inc., New York, 1956, 428 pp. (pp. 27-30).
10. U.S. Weather Bureau, *Daily Series, Synoptic Weather Maps*, Part I and Part II, 1955 and 1956.
11. U.S. Weather Bureau, "Normal Weather Charts for the Northern Hemisphere," *Technical Paper No. 21*, Washington, D.C., 1952.

[Received April 23, 1964; revised September 11, 1964]